DE-AC22-92PC91346-10

DEVELOPMENT OF THE INTEGRATED ENVIRONMENTAL CONTROL MODEL:

Performance Model for the NOXSO Process ~~(DRAFT)~~

Quarterly Progress Report

to

Pittsburgh Energy Technology Center
U.S. Department of Energy
Pittsburgh, PA 15236

from

Center for Energy and Environmental Studies
Carnegie Mellon University
Pittsburgh, PA 15213

Prepared by

Jayant R. Kalagnanam
Edward S. Rubin

April 1995

MASTER

Table of Contents

1.0 Introduction

The purpose of this contract is to develop and refine the Integrated Environmental Control Model (IECM) created and enhanced by Carnegie Mellon University (CMU) for the U.S. Department of Energy's Pittsburgh Energy Technology Center (DOE/PETC) under contract Numbers DE-FG22-83PC60271 and DE-AC22-87PC79864.

In its current configuration, the IECM provides a capability to model various conventional and advanced processes for controlling air pollutant emissions from coal-fired power plants before, during, or after combustion. The principal purpose of the model is to calculate the performance, emissions, and cost of power plant configurations employing alternative environmental control methods. The model consists of various control technology modules, which may be integrated into a complete utility plant in any desired combination. In contrast to conventional deterministic models, the IECM offers the unique capability to assign probabilistic values to all model input parameters, and to obtain probabilistic outputs in the form of cumulative distribution functions indicating the likelihood of different costs and performance results.

The most recent version of the IECM, implemented on a Macintosh II computer, was delivered to DOE/PETC at the end of the last contract in May 1991. The current contract will continue the model development effort to provide DOE/PETC with improved model capabilities, including new software developments to facilitate model use and new technical capabilities for analysis of environmental control technologies. Integrated environmental control systems involving pre-combustion, combustion, and post-combustion control methods will be considered.

The work in this contract is divided into two phases. Phase I involves developing the existing modules of the IECM and training PETC personnel on the effective use of the model. Phase II deals with creating new technology modules, linking the IECM with PETC databases, and training PETC personnel on the use of the updated models.

The present report summarizes recent progress on the Phase I effort during the period January 1 - March 31, 1995. In particular, this report gives a preliminary summary of the new performance model developed for the NOXSO process . The performance model is developed from first principles and parametrized based on experimental data from pilot plants. This model is to be used in the IECM for conceptual designs of planned new commercial scale installations.

2.0 Background to the NOXSO Process

The NOXSO process is an advanced technology that removes both SO_2 and NO_x simultaneously using a sorbent prepared by spraying sodium carbonate on the surface of γ-alumina spheres. It is designed to achieve SO_2 removal efficiencies above 90% and NO_x removal at levels above 80%. The main features of this process are:

i) Simultaneous SO_2 and NO_x removal in a single absorber vessel;
ii) regenerative use of sorbent thereby avoiding the production of liquid or solid waste; and
iii) production of a saleable byproduct in the form of sulfur or sulfuric acid.

The key differences between the NOXSO process and the Copper Oxide (CuO) process (another integrated emission control technology) are twofold:

i) NOXSO uses a sorbent that consists of sodium carbonate sprayed on the surface of γ-alumina spheres while the CuO process uses copper oxide as a sorbent. The latter requires operation at high temperatures upstream of the air preheater, whereas the NOXSO catalyst operates at lower temperatures downstream of the preheater.

ii) NOXSO recycles the NO_x removed from the flue gas back to the furnace along with combustion air. By injecting it into the fuel-rich high temperature combustion zone it is decomposed to N_2 and O_2. The CuO process, on the other hand, requires the use of ammonia as an additional reagent to reduce NO_x to N_2.

The NOXSO process was developed in the early 1980s and successfully demonstrated at the small-scale (0.17 MW) in 1983-85 at TVA's Shawnee Steam Plant facility (Haslbeck & Neal, 1985; Yates, 1983). This was followed by Process Development Unit (PDU) tests on a slightly larger scale (0.75 MW) in cooperation with DOE/PETC in the mid-eighties. A Life-Cycle Test Unit (LCTU) was built (0.06 MW) in 1988 to examine the NOXSO process in an integrated continuous mode operation (Yeh, Drummond, Haslbeck, & Neal, 1987; Yeh, Ma, Pennline, Haslbeck, & Gromicko, 1990). Finally a Proof-of-Concept (POC) unit was built in the early 1990s at a 5 MW scale as the last test before full-scale demonstration (Black, Woods, Friedrich, & Leonard, 1993; Ma, 1994-95; Ma, Haslbeck, et. al., 1993). Based on these tests, conceptual designs of commercial scale units are now being developed.

2.1 Study Scope and Objectives

This report provides a description of the NOXSO process and refines the existing performance models in the literature and in the IECM computer model. Special attention is given to the fact that no installations currently exist at a commercial size of 200 MW or greater. This lack of information at a large scale introduces additional uncertainty and requires that models parametrized using data from pilot plants of about 5 MW be extrapolated. The process model presented in this report uses principles of thermodynamics and mass transfer for unit operations of the NOXSO process. These models are then parametrized using data from pilot scale studies and subsequently used for conceptual design of planned commercial size plants.

The accuracy of model predictions depends in large part on how completely all the relevant processes have been modeled. Past experience in industry has shown that mass transfer units, especially for solid-gas and liquid-gas exchange, are difficult to scale up. This can lead to uncertainty in predicting the performance of commercial-scale installations. In this report, process performance models developed by NOXSO Corporation, which have been parametrized against Proof-of-Concept (POC) data have been used. These process models were then integrated into the IECM framework to provide an overall system model for the NOXSO process in which uncertainties can be modeled explicitly.

2.2 Organization of Report

This report is organized as follows: Section 3 provides a description of the unit operations used in the NOXSO process. Section 4 provides some theoretical background for modeling fluidized beds. Section 5 provides mass balance models for all NOXSO process areas along with emission control design equations for the adsorber and regenerator. Section 5 also provides a numerical example illustrating the use of these models for conceptual design of a commercial scale NOXSO plant.

3.0 Process Description

A schematic of the NOXSO process is shown in Figure 1. It consists of four main units: the adsorber, sorbent heater, regenerator, and the sorbent cooler. SO_2 and NO_x are adsorbed from the flue gas onto the surface of the sorbent at 320° F in a single-stage fluidized bed adsorber. The SO_2 reacts with the sodium bicarbonate on the sorbent surface to form sodium sulfates. The sorbent is then transported into the three-stage fluidized bed sorbent heater using a dense-phase conveyer, where it is heated to 1150° F to desorb NO_x. The desorbed NO_x is recycled to the furnace where about 65% is reduced to N_2. Following NO_x desorption, the sorbent is transported via a J-valve to a regenerator where natural gas and steam are used to reduce the sulfate on the sorbent to SO_2 and H_2S which are also desorbed. These offgases are sent to a Claus plant or a sulfuric acid plant to recover the sulfur. Finally, sorbent is transported to a three-stage fluidized bed cooler (via a second J-valve) where it is cooled to 320° F and transported back to the adsorber via a third J-valve.

Provided in the following sections is a brief description of each unit operation along with its associated process chemistry. Discussion regarding the modeling of the mass transfer operations for each unit can be found in Section 5.

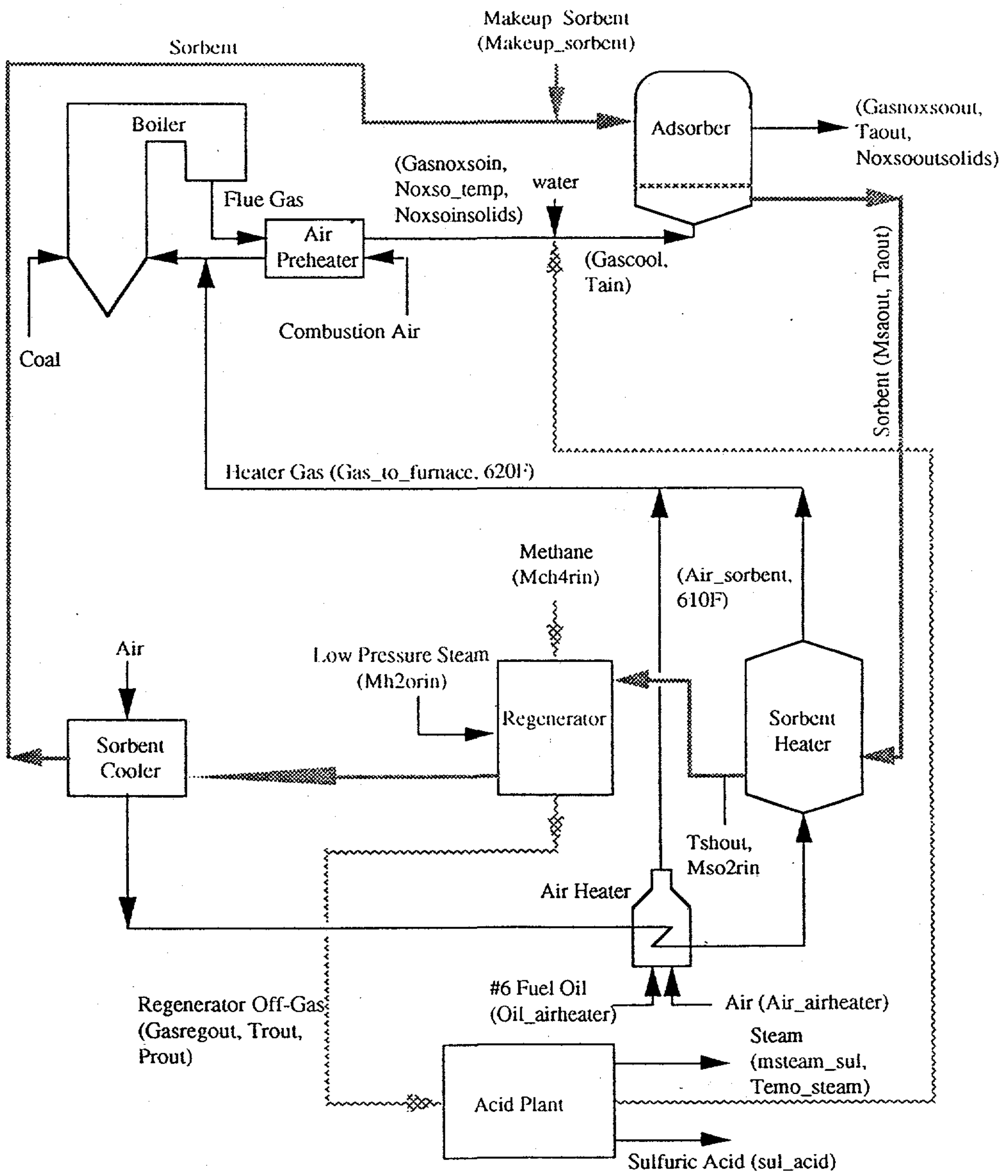

Figure 1. A schematic of the NOXSO process flowsheet

3.1 Adsorber

The adsorber consists of a single-stage fluidized bed containing the Na_2CO_3 covered γ-alumina beads of 1/16 inch diameter. The operating temperature of the bed is 320° F at which temperature Na_2CO_3 is reduced to Na_2O. If necessary, the flue gas is first cooled to 320° F by spraying water into the flue gas ducts. It then passes through the adsorber at a superficial velocity at least as large as the minimum fluidization velocity. The SO_2 and NO_x in the flue gas are adsorbed onto the surface of the alumina beads via solid-gas mass transfer.

Based on laboratory experiments and the results obtained from the POC tests the proposed mechanism for the SO_2/NO_x adsorption is as follows:

$$Na_2O + SO_2 \Leftrightarrow Na_2SO_3 \tag{1}$$

$$Na_2SO_3 + 1/2\ O_2 \Leftrightarrow NaSO_4 \tag{2}$$

$$Na_2O + SO_2 + NO + O_2 \Leftrightarrow Na_2SO_4 + NO_2 \tag{3}$$

$$Na_2O + 3\ NO_2 \Leftrightarrow 2\ NaNO_3 + NO \tag{4}$$

The overall reaction summarizing (1) and (2) is given by:

$$Na_2O + SO_2 + 1/2\ O_2 \Leftrightarrow NaSO_4 \tag{5}$$

The overall reaction summarizing (3) and (4) is given by:

$$4\ Na_2O + 3\ SO_2 + 2\ NO + 3\ O_2 \Leftrightarrow 3\ Na_2SO_4 + 2\ NaNO_3 \tag{6}$$

Examining reactions (5) and (6), we see that 1.5 moles of SO_2 are adsorbed for every mole of NO. The rate of reactions for both SO_2 and NO_x adsorption have been established as first-order based on experimental data. Therefore, the reaction rate is:

$$\frac{dC_i}{dt} = -k_i\,[C_i]\,S$$

where k_i is the reaction rate constant, $[C_i]$ is the concentration of SO_2 or NO_x, and S is the available surface area of the sorbent. The available surface area depends on the gas-solid mixing and flow conditions in the fluidized bed. Modeling the flow in a fluidized bed is quite complex and often difficult, therefore, the available surface area is usually experimentally determined.

3.2 Sorbent Heater

The saturated sorbent from the bottom bed of the adsorber is transported to the top of the sorbent heater using a dense phase conveyor system. The sorbent heater is a three-stage fluidized bed reactor. A natural gas fired air heater supplies hot air to heat the sorbent to 1150° F. During the heating process all of the NO_x (65%-75% NO_2, balance NO) and some of the SO_2 desorbs from the sorbent. In commercial applications the heater off-gas, which is rich in NO_x, is returned to the furnace. The introduction of NO_x recycle into the furnace results in: (a) inhibited NO_x production due to higher NO_x concentrations, and (b) reduction of NO_x to N_2. As noted earlier, about 65% of the recycled NO_x is reduced to N_2.

NO_x desorbtion in the sorbent heater produces both NO and NO_2, where the latter is about 65-75% of the total NO_x. The type of gas used (i.e., the constituents of hot air plus combustion byproducts) to heat the sorbent does not affect the ratio of NO to NO_2 (in NO_x) significantly. A small fraction of SO_2 is also desorbed. Based on experimental findings the following reaction mechanisms have been proposed to explain the desorbtion process:

$$2\,NaNO_3 \rightarrow Na_2O + 2\,NO_2 + 1/2\,O_2 \qquad (7)$$

$$2\,NaNO_3 \rightarrow Na_2O + NO_2 + NO + O_2 \qquad (8)$$

$$Na_2SO_3 \Leftrightarrow Na_2O + SO_2 \qquad (9)$$

Fluidized bed reactors have excellent heat transfer properties, and it has been experimentally observed that all of the adsorbed NO_x is desorbed in the sorbent heater. In this work, the sorbent heater is modeled purely as a heat and mass transfer device resulting in 100% NO_x removal and 0-5% SO_2 removal.

3.3 Regenerator

The regenerator is of a moving bed type, i.e., the sorbent continuously moves from the top to the bottom of the regenerator bed. The hot sorbent from the bottom of the sorbent heater is transported to the top of the regenerator via J-valves. Natural gas is used to treat the hot sorbent and reduce the sulfate to SO_2, H_2S, and sulfide. In the lower part of the regenerator bed steam is used to hydrolyze any residual sulfide to H_2S. The off-gas streams from the natural gas treater and steam treater are mixed and fed either to a Claus plant, which converts gases to elemental sulfur, or to a sulfuric acid plant.

The reaction mechanisms for regeneration of the sorbent based on POC results are as follows:

$$1/4\ CH_4 + Na_2SO_4 \rightarrow 1/4\ CO_2 + SO_2 + 1/2\ H_2O + Na_2O \tag{10}$$

$$SO_2 + Na_2O \rightarrow Na_2SO_3 \tag{11}$$

$$3/4\ CH_4 + Na_2SO_3 \rightarrow 3/4\ CO_2 + H_2S + 1/2\ H_2O + Na_2O \tag{12}$$

$$Na_2S + H_2O \Leftrightarrow H_2S + Na_2O \tag{13}$$

$$CO_2 + Na_2S \rightarrow COS + Na_2O \tag{14}$$

$$1/2\ CO_2 + Na_2S \rightarrow 1/2\ CS_2 + Na_2O \tag{15}$$

Equations 10, 11, and 12, represent the regeneration in the upper part of the moving bed, and can be summarized as follows:

$$CH_4 + Na_2SO_4 \rightarrow CO_2 + H_2S + H_2O + Na_2O \tag{16}$$

The residual sulfide is hydrolized in the lower part of the moving bed:

$$3\ Na_2S + H_2O + 1.5\ CO_2 \rightarrow 3\ Na_2O + H_2S + COS + 1/2\ CS_2 \tag{17}$$

The reaction rates are governed by the available surface area and the reaction rate constants can be determined experimentally.

3.4 Sorbent Cooler

The sorbent from the regenerator flows into a three-stage fluidized bed sorbent cooler via a second J-valve. The sorbent is cooled to 320° F using ambient air supplied by a fan. The heat is recovered by using the air for combustion in the air heater. The cooled and regenerated sorbent is recycled back to the adsorber via a third J-valve. The cooling of the regenerated sorbent does not involve any chemical reactions and is modelled purely as a heat transfer operation.

4.0 Fluidized Bed Reactors

Fluidizing a bed of solid particles with gas provides a means of bringing the two into intimate contact and thus enhancing mass and heat transfer. The heat transfer properties of fluidized beds are excellent and even when accommodating strongly exothermic or endothermic reactions, the beds remain isothermal due to good solids mixing. Additionally, because of their liquid-like properties, fluidized beds can be mechanically transferred by pumping from one container to another. In many industrial processes the gas mixing in a fluidized bed often is not good due to gas bubbles, which can severely reduce the contact between gas and solids. There can also be problems with particle attrition and break-up caused by the vigorous agitation of particles and their impingement on vessel walls. Often, however, the advantages outweigh the disadvantages and the use of fluidization in industrial processes is fairly common.

In designing a fluidized bed reactor two main factors are considered: (1) the formation of bubbles in the fluidized bed, which is determined by the minimum fluidization velocity U_{mf}, and (2) reactive mass transfer in the fluidized bed. In the following paragraphs models for the calculation of U_{mf} and for reactive mass transfer for fluidized bed reactors are described (Davidson & Harrison, 1971; Kunii & Levenspiel, 1969; Yates, 1983).

4.1 Minimum Fluidization Velocity

Fluidization of a bed with solid particles occurs when the superficial gas velocity in a vessel is large enough so that the drag force on the particles equals the gravitational pull of the particle. At this velocity, called the minimum fluidization velocity, U_{mf}, the bed takes on the appearance of a fluid with a flat surface responding in the same way as a fluid to stirring or pouring. If the superficial gas velocity increases above U_{mf}, bubbles form in the bed and rise to the surface where they burst through in the same way as gas bubbles in a boiling liquid. At these velocities the bed is essentially divided into two phases — the dense or emulsion phase where the gas percolates through as in a packed bed, and the lean or bubble phase where much of the gas is not in contact with the solids. If the superficial velocity is increased further the gas bubbles increase in size and might become as large as the diameter of the container itself. The bed is then said to be "slugging" and is characterized by considerable heaving of the surface.

The expressions available for estimating U_{mf} in terms of the physical properties of the solid particles and the fluidizing gas are based on the principle of taking a gas velocity-pressure drop relationship and extending it to the point where particles become fluidized and the gas velocity is U_{mf}. The Ergun equation (Yates, 1983) provides an expression for pressure drop through a vertical bed of particles (for size > 150 μm) of height H_{mf}:

$$\frac{\Delta p}{H_{mf}} = \frac{150\,(1-\varepsilon)^2}{\varepsilon^3} \times \frac{\mu \times V}{(\psi\, d_p)^2} + \frac{1.75\,(1-\varepsilon)}{\varepsilon^3} \times \frac{\rho_g\, V^2}{\psi\, d_p} \tag{18a}$$

where

$$Re_{mf} \equiv \frac{V_{mf}\, d_p\, \rho_g}{\mu}$$

$$Ga \equiv \frac{d_p\, \rho_g\, (\rho_s - \rho_g)\, g}{\mu^2}$$

4.2 Fluidized Bed Reactor Modeling

Modeling a fluidized bed reactor is critical for evaluating design parameters such as sorbent residence time and sorbent flow rate. The performance of the fluidized bed reactor is determined by a combination of chemical factors and hydrodynamic factors. The chemical factors are determined by the reaction kinetics and the stochiometry of the reaction. The hydrodynamic factors are determined by the gas distribution, bubble size and residence time, and the interphase exchange rate. In order to quantify the way in which these factors affect the reactor performance we present a model based on the theory of two-phase flow in fluidized beds which makes explicit the contribution of these factors.

Most reactor models assume that if the superficial velocity is greater than U_{mf} then the gas entering the bed divides into two streams, one flowing through the emulsion phase and the other flowing as bubbles. Gas flowing in the emulsion phase is in intimate contact with the solid particles so the reaction can proceed efficiently. Bubbles, however, are essentially empty of particles and gas within them can only react at the walls of the bubble. However, there is an exchange of gas between the emulsion and bubble phase, the bubbles thereby acting as a secondary source of fresh reactant as they rise through the bed. A general one-dimensional two-phase flow model is shown in Figure 2.

For an irreversible, first-order gas-solid reaction with no accompanying volume change, a mass balance for the emulsion phase (Equation 21) and bubble phase (Equation 22) is written as follows:

$$V_e \frac{dy_{Ae}}{dz} + K_{be}\,(y_{Ae} - y_{Ab}) + k_e\, y_{Ae}\, S = 0 \tag{21}$$

$$V_b \frac{dy_{Ab}}{dz} + K_{be}\,(y_{Ab} - y_{Ae}) = 0 \tag{22}$$

where

$V \equiv$ velocity

$y_A \equiv$ concentration of species A

$K_b \equiv$ interphase mass transfer rate per unit volume of bubble gas

$k \equiv$ reaction rate constant

$S \equiv$ surface area of solid available for reaction

The subscript 'e' is used for emulsion phase and subscript 'b' is used for bubble phase. These equations have been simplified using the following assumptions: (i) the reactor operates in steady state, (ii) the gas is in plug flow in both phases and hence there is no back-flow, and (iii) no chemical reaction occurs in the bubble phase.

These model formulations provide an alternative form to the models described below in Section 5. An advantage is that this formulation explicitly recognizes the two separate phases, especially the bubble phase which may limit performance in future process scale-up. Further development of Equations 21 and 22 will appear in future reports on this project.

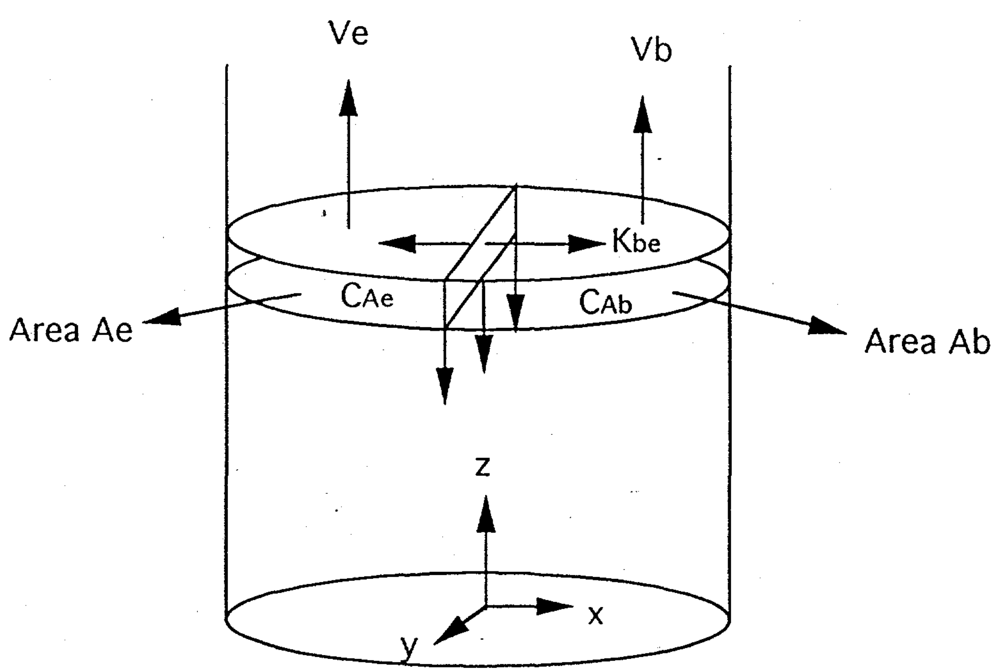

Figure 2. The general one-dimensional two-phase flow

5.0 NOXSO Process Performance Model

The four main process areas for the NOXSO process were described in Section 3. Across these areas, the adsorber, sorbent heater, and sorbent cooler use a fluidized bed for improved gas-solid contact. The sorbent heater and sorbent cooler utilize a fluidized bed mainly for efficient heat transfer between gas and solid sorbent particles. As discussed in Section 3, the fluidized bed provides excellent heat transfer properties and provides isothermal conditions. The adsorber, on the other hand, is used primarily for reactive mass transfer, involving pollutant removal. The modeling of the adsorber performance will be discussed in some detail. The regenerator is a moving bed reactor which is used for regenerating sulfur. The reactive mass transfer model for this unit also is treated in some detail. Since a number of equations and variables are introduced the nomenclature used is described at the end of the document. To the extent possible, the nomenclature used here is identical to that tsed in NOXSO Corporation reports, so as to facilitate comparisons with source materials.*

5.1 Fluid Bed Adsorber Model

A mathematical model based on first principles has been developed by NOXSO Corporation for the design of future commercial installations (Ma and Haslbeck, 1993). The reaction rate constants for SO_2 and NO_x sorption were derived using data from the PDU, LCTU, and POC tests. The rate constants have been lumped to treat the hydrodynamics of the gas-solid contact and the reaction kinetics in one variable. The main purpose of this model is to provide design equations for calculating key design parameters such as sorbent inventory and sorbent residence time for a desired level of SO_2 and NO_x removal. We have rewritten the equations developed by NOXSO Corporation to provide explicit relations for the design variables. Since the equations are quite detailed, and it is easy to get lost in the nomenclature, we first provide an overview of the equations.

Equations 23-26 express the pollutant removal efficiency in terms of the operating parameters of the fluidized bed (W, Fs) and physical constants (K_i, ρ, etc). The main objective here is to progressively rewrite the equations in terms of variables and functions which are readily measured and can be provided as inputs to the model. Equation 27 and 28 provide a set of equations for removal efficiencies, operating parameters and physical

* Note that this nomenclature differs from that used in other IECM reports. In particular, the symbol ϕ is used in other reports to signify reagent stoichiometry; here it means removal efficiency. The symbol λ used here for stochiometry is equivalent to η in other IECM reports.

constants. Equations 29-32 provide a set of relations for the physical constants determined from experimental data. Finally, Equation 33 provides the design equations for the operating parameters of the fluidized bed absorber.

The fluid bed mass balance in the vertical direction is derived using the following assumptions: (i) there is no bubbling in the fluidized bed, (ii) the gas is in plug flow, (iii) the solids are in mixed flow, and (iv) SO_2 and NO_x absorption are first-order reactions with respect to their concentrations. Therefore the mass balance is written as follows:

$$- V\, C_0\, (y_{oi} - y_{fi}) = \rho\, \lambda_i\, n\, K_i\, P\, \bar{y}_i\, (1 - \bar{X})\, H \tag{23}$$

Notice that unlike Equation 21, the mass balance has been written for the total bed by using a mean value for the concentration of gas species 'i'.

Defining the removal fraction as:

$$\phi_i = \left(1 - \frac{y_{fi}}{y_{oi}}\right)$$

Equation 23 can be rewritten as follows:

$$\phi_i = \frac{W}{F_g} \lambda_i\, n\, K_i\, P\, \frac{\bar{y}_i}{y_{oi}}\, (1 - \bar{X}) \tag{24}$$

When sorption takes place in the adsorber, both SO_2 and NO_x compete for active sites on the sorbent. A mass balance on the sorbent material in a mixed flow reactor results in:

$$F_s\, (\bar{X} - X_0) = W\, P\, (K_1\, \bar{y}_1 + K_2\, \bar{y}_2)\, (1 - \bar{X}) \tag{25}$$

Combining Equations 24 and 25, the removal efficiency for the ith gas species can be rewritten as:

$$\phi_i = \frac{W\, E_i}{F_g} K_i\, P\, \frac{\bar{y}_i}{y_{oi}}\, \frac{1}{1 + \dfrac{W}{F_s} P\, (K_1\, \bar{y}_1 + K_2\, \bar{y}_2)} \tag{26}$$

where $E_i = \lambda_i\, n\, (1 - X_0)$

Since the alumina substrate also adsorbs SO_2 and NO_x from the flue gas, the stochiometric ratio of reactant gas to active sorbent must include contributions from both sodium and alumina. In order to avoid having to make this distinction, an empirical relationship has been developed to calculate the stochiometry as a ratio of adsorber temperature:

$$\begin{aligned} \text{For } SO_2: \frac{1}{\lambda_1} &= 0.3761 + 0.0052 \times T_a \\ \text{For } NO_x: \frac{1}{\lambda_2} &= -4.789 + 0.075 \times T_a \end{aligned} \tag{26a}$$

where T_a is in degrees Celcius.

Since the gas flow in the fluidized bed is assumed to be plug flow and the reaction is first-order, $\bar{y}_i$ can be taken as the logarithmic mean expressed in terms of the removal efficiency as follows:

$$\bar{y}_i = \frac{-y_{oi}\,\phi_i}{\ln(1-\phi_i)}$$

Substituting for $\bar{y}_i$ in Equation 26, the removal efficiencies can be written as follows:

For SO_2:

$$\ln(1-\phi_1) - \frac{W}{F_s} P \frac{A}{A_0}\left(K_1\, y_{01} + K_2\, y_{02}\, \frac{\phi_2}{\ln(1-\phi_2)}\, \frac{\ln(1-\phi_1)}{\phi_1}\right)\phi_1 + \frac{W E_1}{F_g} P K_1 \frac{A}{A_0} = 0 \tag{27}$$

For NO_x:

$$\ln(1-\phi_2) - \frac{W}{F_s} P \frac{A}{A_0}\left(K_2\, y_{02} + K_1\, y_{01}\, \frac{\phi_1}{\ln(1-\phi_1)}\, \frac{\ln(1-\phi_2)}{\phi_2}\right)\phi_2 + \frac{W E_2}{F_g} P K_2 \frac{A}{A_0} = 0 \tag{28}$$

Note that since removal is a sorption reaction, the rate constant is proportional to sorbent surface area which has been introduced into the equations (refer to Section 3.1). Equations 27 and 28 can be solved simultaneously for the removal efficiencies in terms of the following exogenously specified variables :

(i) The key operating parameters of the fluidized bed, i.e., sorbent residence time (W/F_s) and sorbent inventory (W),

(ii) Key inlet conditions including the mole fractions of SO_2 and NO_x (y_{oi}) entering the adsorber, and the flue gas flow rate (F_g),

(iii) Key physical constants including the lumped kinetic constants (K_i), the available surface area (A/A_o), and the available unused sorbent capacity (E_i).

The physical constants have been determined by NOXSO Corporation using experimental data from the PDU, LCTU, and POC tests. In the following paragraphs we describe the parametrizations used for solving the above equations.

The sorbent's SO_2 and NO_x capacities are calculated as follows:

$$\text{For } SO_2\text{: } E_1 = \left(\lambda_1 n + \frac{0.8 - S_r}{3200}\right)\frac{A}{A_0} \tag{29}$$

$$\text{For } NO_x\text{: } E_2 = \left(\lambda_2 n + \frac{0.8 - S_r}{3200}\right)\frac{\lambda_2}{\lambda_1} \tag{30}$$

where $n = \frac{n_{Na}}{2300} - \frac{n_{SiO_2}}{6000}$

The factor 0.8 in Equations 29 and 30 is the average sulfur content (% wt) of the regenerated sorbent in the PDU tests used as a reference for the above parametrization. The temperature dependent rate constants were derived by NOXSO Corporation by using PDU data along with Equations 27 and 28 to solve for K_i at different temperatures. A least squares fit was used to obtain the following relations:

$$\text{For } SO_2\text{: } K_1 = 52.15 \exp\left(\frac{-1840.2}{T_a + 273}\right) \tag{31}$$

$$\text{For } NO_x\text{: } K_2 = 14.75 \exp\left(\frac{-912.14}{T_a + 273}\right) \tag{32}$$

The available surface area A/A_O has a value of 0.6 based on PDU test data collected after sorbent surface area had stabilized.

For designing the adsorber, we need to estimate the operating parameters of the fluidized bed for given removal efficiencies for SO_2 and NO_x. The key parameters are the sorbent circulation rate, sorbent inventory, sorbent residence time and fluidized bed height. Equations 27 and 28 can be solved for sorbent inventory and sorbent circulation rate. Note that sorbent residence time also can be calculated from these two variables.

$$\frac{W}{F_s} = \frac{a_1 b_3 + a_3 b_1}{a_2 b_3 + a_3 b_2} \tag{33a}$$

$$W = \frac{b_1(a_2 b_3 + a_3 b_2) - b_2(a_1 b_3 + a_3 b_1)}{b_3(a_2 b_3 + a_3 b_2)} \tag{33b}$$

where

$$a_1 = \ln(1-\phi_1); \quad b_1 = \ln(1-\phi_2);$$

$$a_2 = P\frac{A}{A_0}\left(K_1 y_{01} + K_2 y_{02} \frac{\phi_2}{\ln(1-\phi_2)} \frac{\ln(1-\phi_1)}{\phi_1}\right);$$

$$b_2 = P\frac{A}{A_0}\left(K_2 y_{02} + K_1 y_{01} \frac{\phi_1}{\ln(1-\phi_1)} \frac{\ln(1-\phi_2)}{\phi_2}\right);$$

$$a_3 = \frac{E_1}{F_g} P K_1 \frac{A}{A_0}; \quad b_3 = \frac{E_2}{F_g} P K_2 \frac{A}{A_0};$$

The total pressure drop in the fluidized bed is easily calculated by considering the total weight of sorbent that is fluidized by the flue gas, i.e.

$$\Delta p = \frac{W}{A_a}$$

5.2 Regenerator Model

The regenerator consists of two sections as shown in Figure 3. The sorbent moves down in a moving bed, while the regenerating gases move upward. The flow is assumed to be approximately plug flow. Natural gas enters the bottom of the upper section of the regenerator and reduces the sulfate on the sorbent to SO_2, H_2S, and sulfide. SO_2 and H_2S evolve as gases and sulfide remains on the sorbent surface. Steam is introduced in the lower section of the regenerator and hydrolyzes the sulfide to H_2S.

The models presented here determine the main operating parameters of the regenerator which are the sorbent residence times for natural gas reduction and steam reduction. Equation 34 provides a mass balance for sulfur which has been used as a basis for interpreting experimental data. Equation 35 provides the rate constants for the two reduction reactions given by Equations 16 and 17. Finally, Equation 35 provides the design equations for sorbent residence times.

The sulfur molar balance provides the rate of sulfur regeneration as a function of sorbent flow rate and sorbent inventory as follows:

$$F_s\, S_a\, dX_r = r_s\, dW \Rightarrow X_r = \frac{W}{F_s\, S_a}\, r_s \tag{34}$$

where $X = 1 - S / S_a$

The sulfur regeneration rate has been studied extensively in the POC plant. The experimental results indicate that regeneration consists of two main reactions and both are first-order with respect to sorbent sulfur content. The first set of reactions, corresponding to Equation 16, uses natural gas to reduce the sulfate. The second reaction corresponds to Equation 17 and uses steam to hydrolyze sulfide on the sorbent surface. Data from the POC plant was plotted as X_r vs. $W/(F_S\ S_a)$ based on Equation 30. This plot consists of two straight lines with different slopes. The lines correspond to the reaction rates of Equations 16 and 17, respectively. *The reaction rate of Equation 16 is eight times higher than that of Equation 17.* The reaction rates have been parametrized using experimental data from the POC tests, and are given as follows (Ma and Haslbeck, 1993):

$$r_{s_1} = k_1 \exp\left(-\frac{E_1}{RT}\right) S_a \tag{35a}$$

$$r_{s_2} = k_2\,(1 - 0.6)\, S_a \tag{35b}$$

$$\frac{E}{R} = 34554.0$$

$$\ln(k_1) = 38.97$$

$$k_2 = 0.85$$

$$S_a = 0.01$$

Another result of these experimental studies is that 60% of the sulfur on the spent sorbent is regenerated by natural gas, while the steam treatment regenerates 20-30% of the remaining sulfides on the sorbent. The shift in sulfur regeneration from reaction 1 to reaction 2 at $X_{shift} = 0.6$ is independent of the inlet sorbent temperature. However, the amount of sulfur that is regenerated by the steam treater (X_{final}) depends on the inlet sorbent temperature. Typically, varying the inlet temperature from 1150-1250 F increases the sulfur regeneration from 20% to 30%. Assuming a linear relationship, this is written as:

$$X_{final} = (0.001\ T - 0.35 - X_{shift}) \tag{36}$$

The heat of regeneration for both reactions also has been estimated from experimental data:

$$\Delta H_1 = 917.2 \text{ Btu/lb sulfur}$$

$$\Delta H_2 = 2032 \text{ Btu/lb sulfur}$$

The design equations for sorbent residence times are now straightforward:

$$t_{CH_4} = \frac{X_{shift} \times S_a}{r_{s_1}} \tag{37a}$$

$$t_{H_2O} = \frac{(X - X) \times S_a}{r_{s_2}} \tag{37b}$$

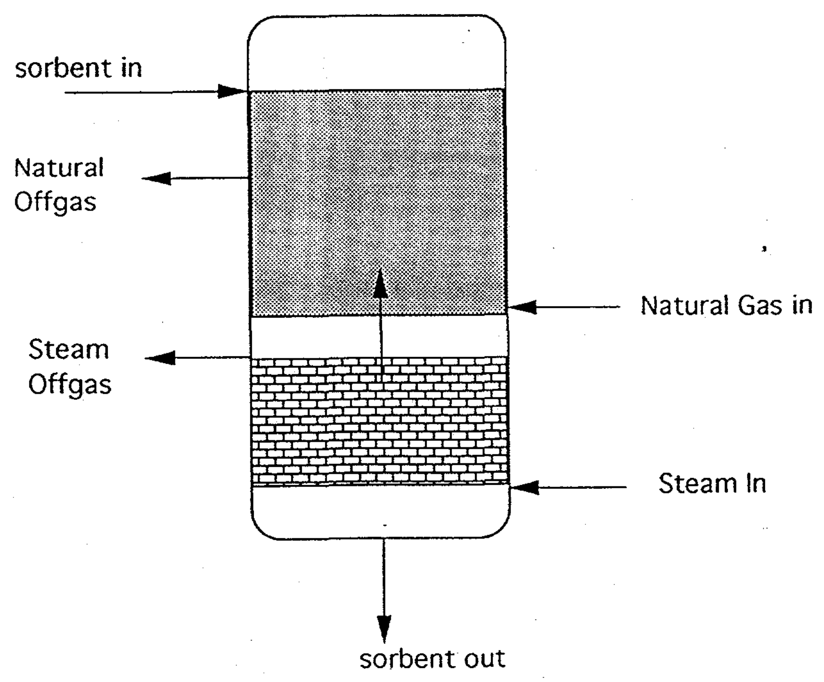

Figure 3. Schematic of the NOXSO Regenerator

5.3 Sorbent Heater and Cooler

Models of the sorbent heater and cooler are limited to simple mass and energy balances. The NO_x is completely desorbed in the regenerator and about 8-10% of the SO_2 is desorbed. The heat exchange between the sorbent and the hot air is treated as a simple energy balance. Similarly, the cooling of the sorbent in the sorbent cooler is also treated as a simple energy balance are as follows:

$$\mp F_g C_p (T - T_0) = \pm Fs\, c_{Ps} (Ts - T_{S0}) \pm UA_w (T - T_a)$$

where

F_g	gas flow rate (kmole/sec)
c_p	gas specific heat kcal/mole(°C)
F_s	sorbent flow rate (kg/sec)
c_{p_s}	sorbent heat capacity (kcal/kg°C)
T_s	sorbent temperature (°C)
U	wall heat transfer coefficient (kcal/m^{2}sec)
A_w	vessel wall surface area, (m^2)
T_A	ambient air temp. (°C)

The subscript "0" refers to initial condition.

The $\pm$ signs are chosen depending on whether sorbent is being cooled or heated. Usually, the vessel walls of the heat exchanger are insulated to keep heat transfer to ambient air low.

5.4 A Numerical Example

Provided here is a conceptual design of a commercial NOXSO plant of size 300 MW achieving 90% SO_2 removal and 80% NO_x removal. The coal used is a medium sulfur Appalachian coal (2.6% sulfur, and 1.12% nitrogen). The design specifications are:

Size:	300 MW, 725 Kacfm (at 320° F)
Temp. of flue gas entering adsorber	320° F
SO_2 removal	90%
NO_x removal	80%
Inlet SO_2 conc. (η_{SO2})	2120 ppm (calculated by IECM)
Inlet NO_x conc. (η_{NOx})	420 ppm (calculated by IECM)
Sorbent	Na_2CO_3 on γ-alumina spheres

Actual Removal Efficiencies

Since some NO_x and SO_2 are recycled back to the boiler, we need to calculate the actual removal efficiencies required to achieve the desired design. This can be calculated by a simple mass balance of SO_2 and NO_x around the power plant once the recycle fractions are known. Based on the current NOXSO design, these fractions are 94% for SO_2 and 65% for NO_x. Thus,

$$\phi_1 = \frac{\eta_{SO_2}}{R_{SO_2} \times \left(1 + \frac{1 - R_{SO_2}}{R_{SO_2}} \times \eta_{SO_2}\right)} = \frac{0.9}{0.94 \times \left(1 + \frac{1 - 0.94}{0.94} \times 0.9\right)} = 90.5\%$$

$$\phi_2 = \frac{\eta_{NO_x}}{R_{NO_x} \times \left(1 + \frac{1 - R_{NO_x}}{R_{NO_x}} \times \eta_{NO_x}\right)} = \frac{0.8}{0.65 \times \left(1 + \frac{1 - 0.65}{0.65} \times 0.8\right)} = 86.0\%$$

Adsorber

Physical parameters required for the calculations are first estimated. Substituting the adsorber temperature (in °C) in Equation 26a we estimate the stochiometric ratios

$$\lambda_1 = 0.93; \; \lambda_2 = 0.19.$$

Similarly, the temperature-dependent rate constants are obtained from Equations 31 and 32 are:

$$K_1 = 0.5734 \text{ (atm sec)}^{-1}; \; K_2 = 1.577 \text{ (atm sec)}^{-1}.$$

The sorbent capacities are calculated using Equations 29 and 30. Based on pilot plant data, the weight fraction of sodium in the sorbent is taken to be 3.8%, the sulfur content of regenerated sorbent is 0.25%, and the available surface area fraction is 0.6. Thus,

$$\text{For } SO_2 : E_1 = \left(\lambda_1 n + \frac{0.8 - S_r}{3200}\right)\frac{A}{A_0} = \left(0.93 \times 1.65 \times 10^{-3} + \frac{0.8 - 0.25}{3200}\right) \times 0.6 = 1.02 \times 10^{-3}$$

$$\text{For } NO_x : E_2 = \left(\lambda_2 n + \frac{0.8 - S_r}{3200}\right)\frac{\lambda_2}{\lambda_1} = \left(0.19 \times 1.65 \times 10^{-3} + \frac{0.8 - 0.25}{3200}\right) \times \frac{0.93}{0.19} = 0.3 \times 10^{-3}$$

Now the key operating parameters, sorbent inventory and sorbent residence time, can be calculated using Equation 33. The calculation of the intermediate variables is not shown.

$$\frac{W}{F_s} = -\frac{a_1\, b_3 + a_3\, b_1}{a_2\, b_3 + a_3\, b_2} = -\frac{-2.3\times 10.4\times 10^{-6} - 11.2\times 10^{-6}\times 1.61}{1.08\times 10^{-3}\times 10.4\times 10^{-6} + 11.2\times 10^{-6}\times 0.7\times 10^{-3}} = 36.6 \text{ min.}$$

$$W = \frac{b_1 - b_2\times W/F_s}{b_3} = \frac{1.61 - 0.7\times 10^{-3}\times 2197}{10.4\times 10^{-6}} = 303{,}700 \text{ lbs}$$

Regenerator

Once again we first evaluate the reaction rates are evaluated using Equation 35.

$$r_{s_1} = k_1 \exp\left(-\frac{E_1}{RT}\right) S_a = \exp(38.97 - 34554/895)\times 0.01 = 0.0138 \text{ lb sulfur/lb sorbent/hr}$$

$$r_{s_2} = k_2\,(1-0.6)\, S_a = 0.85\times 0.4\times 0.01 = 0.0034 \text{ lb sulfur/lb sorbent/hr}$$

The shift in the reducing reaction from methane to water is at X_{shift}=0.6 and X_{final}=0.8. Therefore the residence time of the sorbent is calculated as follows using Equation 37:

$$t_{CH_4} = \frac{X_{shift}\times S_a}{r_{s_1}} = \frac{0.6\times 0.01}{0.0138}\times 60 = 26 \text{ min}$$

$$t_{H_2O} = \frac{(X_{final} - X_{shift})\times S_a}{r_{s_2}} = \frac{0.2\times 0.01}{0.0034}\times 60 = 35 \text{ min}$$

Nomenclature for Section 5

A available surface area of sorbent
A_a cross sectional area of adsorber
A_0 available surface area of fresh sorbent
C_0 molar gas concentration of flue gas, kmole / m^3
F_g flue gas flow rate, kmole / sec
F_s sorbent circulation rate, kg / sec
H height of fluidized bed
ΔH_i heat of reaction for regeneration, Btu / lb sulfur
K rate constant of i^{th} gas species, 1 / (atm sec)
n sodium content on sorbent, kmole / kg sorbent
n_{Na} sodium content on sorbent, %wt
n_{SiO_2} silicon content on sorbent, %wt
P gas pressure, atm
r sulfur regeneration rate, (lb sulfur) / hr / (lb sorbent)
R_{NO_x} fraction of NO_x converted to N in combustor
R_{SO_2} fraction of SO_2 retained on sorbent after heating in sorbent heater
S sulfur fraction of regenerated sorbent, %wt
S_a sulfur fraction of spent sorbenr, %wt
t_i sorbent residence time in regenerator for gas i
T_a temperature of adsorber, °C
V superficial gas velocity
W sorbent inventory, kg
$\overline{X}_a$ mean conversion factor of active sorbent
X_a conversion factor of active sorbent at adsorber inlet
X_r conversion factor for sorbent regeneration
X_{shift} conversion factor at which regeneration shifts
X_{final} total temp. conversion for sorbent regeneration
y_{oi} mole fraction of i^{th} gas species, $z = 0$
y_{fi} mole fraction of i^{th} gas species, $z = H$
$\overline{y}$ mean mole fraction

Greek Symbols

ρ sorbent density in fluid bed, kg / m^3
λ_i stochiometric ratio of i^{th} gas species to active sorbent,
ϕ removal fraction

References

Black, J. B., Woods, M., Friedrich, J. J., & Leonard, C. A. (1993). The NOXSO Clean Coal Technology Project: Commercial Plant Design. In The Thirteenth EPRI/EPA/DOE SO2 Control Symposium, . Boston, MA:

Davidson, J. F., & Harrison, D. (Ed.). (1971). Fluidization. London, UK: Academic Press.

Haslbeck, J. L., & Neal, L. G. (1985). The NOXSO Process Development: An Update. In Ninth EPA/EPRI Symposium on Flue Gas Desulfurization, . Cincinnati, OH:

Kunii, D., & Levenspiel, O. (1969). Fluidization Engineering. New York: Wiley.

Ma, W. T. (1994-95). Performance Modeling of the NOXSO Process. In

Ma, W. T., Haslbeck, J. L., et al., (1993). Proof-of-Concept Testing of the Advanced NOXSO Flue Gas Cleanup Process No. DE-AC22-89PC88889). U.S. Dept. of Energy.

Yates, J. G. (1983). Fundamentals of Fluidized-bed Chemical Processes. Boston, MA: Butterworths.

Yeh, J. T., Drummond, C. J., Haslbeck, J. L., & Neal, L. G. (1987). The NOXSO Process: Simultaneous Removal of SO2 and NOx from Flue Gas. In Spring National Meeting of the AIChE, . Houston, TX:

Yeh, J. T., Ma, W. T., Pennline, H. W., Haslbeck, J. L., & Gromicko, F. N. (1990). Integrated Testing of the NOXSO Process: Simultaneous Removal of SO2 and NOx from Flue Gas. In AIChE Spring National Meeting, . Orlando, FL: